PHYSICAL REVIEW B VOLUME 26, NUMBER 8 15 OCTOBER 1982

Capture and emission of electrons by the resonant state strongly coupled to the lattice in *n*-InSb

L. Dmowski
High Pressure Research Center "Unipress," 01-142 Warsaw, Poland

M. Baj and P. Ioannides*
Institute of Experimental Physics, Warsaw University, Warsaw, Poland

R. Piotrzkowski
High Pressure Research Center "Unipress," 01-142 Warsaw, Poland
(Received 12 November 1981)

The pressure and temperature dependences of the free-electron capture cross section σ and the emission rate α are determined for the defect level which is resonant at ambient pressure and becomes bound at pressures $p > 700$ MPa. Irrespective of the level position, i.e., for the level being resonant as well as bound, both σ and α are thermally activated and their activation energies are the linear functions of pressure. It is found that, during the capture or emission process, the adiabatic potential barrier which originates from the strong defect-lattice coupling cannot be practically tunneled. It means that the barrier is very extensive and the capture or emission process leads to the drastic rearrangement of the defect center in the crystal lattice.

I. INTRODUCTION

This paper refers to the localized defect states which strongly couple to the crystal-lattice vibrations—i.e., the change of the electronic state of the defect induces large lattice relaxation (LLR) around it. LLR is the reason that, for such states, free-carrier capture cross sections are thermally activated and achieve extremely small values at low temperatures. Application of hydrostatic pressure, which markedly changes the thermal ionization energies of strongly localized electronic states, enabled us to investigate capture and emission processes for such a state being resonant as well as bound.

In the present work we used nominally undoped *n*-InSb samples. The measurements of the Hall coefficient versus pressure carried out on such samples by Kończykowski *et al.*[1-3] showed the existence of two different defect levels, called below *A* and *B*, both originating from the same unidentified defect *X*, probably oxygen or a complex with oxygen. In all the investigated samples the concentration of this defect N_x is of the order of 10^{14} cm^{-3}. One of these levels, level *B*, is strongly coupled to the lattice.[3] At atmospheric pressure both levels are resonant ($\epsilon_A = 85$ meV, $\epsilon_B = 140$ meV—related to the bottom of the conduction band).[1] The energies of these levels decrease while the pressure is increased ($\partial\epsilon_A/\partial p = -10.5\times10^{-2}$ meV/MPa, $\partial\epsilon_B/\partial p = -20\times10^{-2}$ meV/MPa, so that at pressures about 800 and 700 MPa, respectively, the levels enter the energy gap. At pressures $p > 700$ MPa level *B* is deeper and therefore, at sufficiently high temperatures, it rules the free-electron concentration. At low temperatures the free-electron capture cross section and the thermal emission rate of this level are enormously small, so that the equilibrium value of the free-electron concentration is achieved with the rate controlled by this level. At temperatures $T \lesssim 77$ K the electron population of the level *B* is practically metastable, while at $T \approx 100$ K the time constant of the kinetics is of the order of minutes.[3,4]

In this paper the capture cross section σ and the emission rate α of level *B* were calculated from the time constant τ, characterizing the free-electron concentration kinetics. Nonequilibrium electron population of the level *B* was obtained by means of sufficiently fast changes of pressure and/or temperature. The measurements of the time-dependent free-electron concentration were carried out using standard electronic transport methods (Hall coefficient as a function of time). In this case the ob-

tained information concerned bulk material and weak electric-field conditions, in the opposition to the capacity methods (thin junction layer in strong electric field). Because the measurements were done at pressures up to 1200 MPa, it was possible to see how the change of the energy of level B (within the range from 140 to -100 meV, relative to the bottom of the conduction band) influences the capture and the emission processes.

II. EXPERIMENTAL RESULTS

Four samples of nominally undoped n-InSb with the free-electron concentration, measured at atmospheric pressure and $T=77$ K ranging from 1.2×10^{14} cm^{-3} to 3.3×10^{14} cm^{-3} and various compensations were used in the experiment. For all the samples the concentration of the X defect centers was $N_x=(1.0-1.4)\times10^{14}$ cm^{-3}. The effective concentration of other, always ionized defects N_d-N_a (where N_d is the concentration of shallow donors and N_a is the concentration of acceptors) for one of the samples was $|N_d-N_a|<5\times10^{12}$ cm^{-3} and for the rest N_d-N_a was higher than 1×10^{14} cm^{-3}. The values of n, N_x, and N_d-N_a for all the samples are given in Table I.

The values of N_d-N_a, as well as the defect concentration N_x, were obtained directly from the experiment: $N_d-N_a=n$ ($p\gg800$ MPa) and $N_x=n(p=1)-n$ ($p\gg800$ MPa)—see Porowski *et al.*[3] For all the samples we measured the time dependence of the Hall coefficients R_H and resistivity ρ, caused by the carrier repopulation, tended to the thermal equilibrium. The measurements were done at various values of hydrostatic pressure up to 1200 MPa and various temperatures within 77—108 K. Nonequilibrium conditions were obtained by means of sufficiently fast changes of external parameters—temperature and/or pressure—which determine equilibrium populations of level B and the conduction band. For R_H and ρ measurements the "double ac" method was used with alternating ($f_1=30$ Hz) sample current and alternating ($f_2=40$ Hz) magnetic field with amplitude $B_0=0.01$ T. The Hall voltage was continuously being measured on f_1+f_2 frequency. The sample was placed in the Cu-Be pressure cell joint with the helium gas compressor by means of a capillary Cu-Be tube. Helium gas, used as a pressure-transmitting medium, ensured that the pressure was always fully hydrostatic. Most of the measurements were done at temperatures 95—108 K. The temperature was stabilized with 0.2-K accuracy. One of the samples $S1$, was also measured at 77 K. At pressure $p<800$ MPa all the measured dependences

$$n(t)=\left|\frac{1}{R_H(t)\,e}\right|$$

were exponential, irrespective of the sample compensation. At $p>800$ MPa for the samples with $N_d-N_a>1\times10^{14}$ cm^{-3} all the $n(t)$ dependences were also practically exponential, while for the sample $S1$ with $|N_d-N_a|<5\times10^{12}$ cm^{-3} they markedly differed from the exponential shape. Figure 1 presents in semilogarithmic scale two typical $n(t)$ dependence—exponential ($p<800$ MPa) and nonexponential ($p>800$ MPa). Every such curve enabled us to calculate the value of the parameter characterizing the free-electron concentration kinetics. This parameter τ, so-called the relaxation time of the free-electron concentration, was defined as

$$\frac{1}{\tau}=-\lim_{n\to n_\infty}\frac{d}{dt}\ln|n(t)-n_\infty|$$

where $n_\infty=\lim_{t\to\infty}n(t)$.

Figure 2 shows for all the samples the relaxation time versus pressure obtained for constant temperature $T=105$ K. Such data allow us to determine the pressure dependence of the free-electron

TABLE I. Values for n, N_x, and N_d-N_a for samples of n-InSb used in experiment.

Sample	n (cm^{-3}) $p=0$, $T=77$ K	N_x (cm^{-3})	N_d-N_a (cm^{-3})
$S1$	1.2×10^{14}	1.2×10^{14}	$<5\times10^{12}$
$S2$	2.8×10^{14}	1.4×10^{14}	1.4×10^{14}
$S3$	3.0×10^{14}	1.0×10^{14}	2.0×10^{14}
$S4$	3.3×10^{14}	1.4×10^{14}	1.9×10^{14}

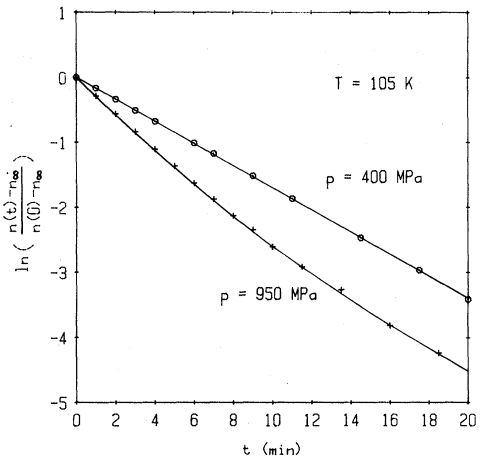

FIG. 1. Two typical time dependences of the free-electron concentration—exponential ($p=400$ MPa) and nonexponential ($p=950$ MPa).

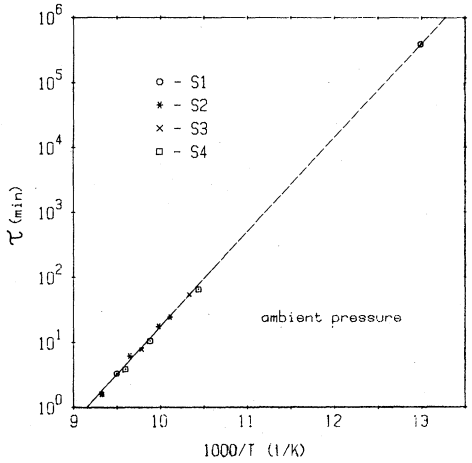

FIG. 3. Dependence of the relaxation time τ upon inverse temperature, measured for all the samples. The solid line is the result of calculations presented in Sec. III.

capture cross section or the emission rate of level B. It is worth pointing out that Fig. 2 presents data for both cases—level B being resonant at $p<700$ MPa, as well as bound at $p>700$ MPa. Because at low pressures level B lies high above the bottom of the conduction band, its equilibrium occupation by electrons is practically equal to zero and therefore it does not depend either on temperature or on pressure. In this case, to observe kinetics, one has to fill level B with electrons by means of the following procedure:

(i) First, the pressure is increased above 800 MPa and then the equilibrium electron population of level B becomes large.

(ii) Next, the temperature is decreased so that the electron population becomes practically metastable and remains high after decreasing the pressure.[3]

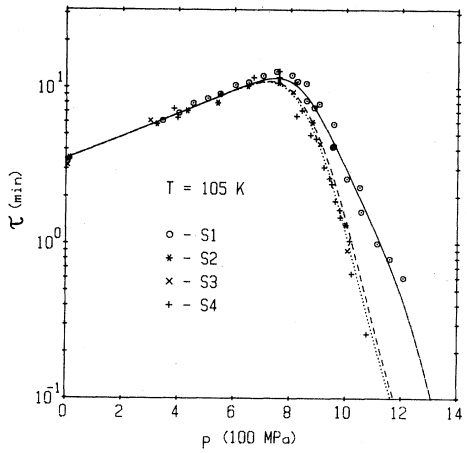

FIG. 2. The pressure dependence of the relaxation time τ measured for all the samples at $T=105$ K. The lines are the results of calculations made for sample $S1$, $S2$, and $S4$, respectively—see Sec. III.

In the low-pressure range the observed kinetics is the emission of electrons ($dn/dt>0$) from level B, which is now degenerate with the conduction band to the conduction band. In the high-pressure range level B is placed in the energy gap and its equilibrium occupation by electrons strongly depends on temperature and pressure. Thus even small but sufficiently fast changes of temperature or pressure initiate the kinetics.[4] In this pressure range both cases $dn/dt>0$ as well as $dn/dt<0$ are possible. For both of them the relaxation time τ is the same. The pressure dependences $\tau(p)$ presented in Fig. 2 are nonmonotonic functions with maximum near to the pressure at which level B enters the energy gap. For pressure $p<800$ MPa, $\tau(p)$ is universal, the same for all the samples. For pressures $p>800$ MPa the differences between relaxation times for different samples reach 1 order of magnitude.

In order to determine the temperature dependence of the free-electron capture cross section (or the emission rate) of level B, we measured the relaxation time τ as a function of temperature for various of pressure as parameter. Figure 3 shows the relaxation time τ versus inverse temperature obtained for all the samples at atmospheric pressure. For sample $S1$ one of the points was obtained at $T=77$ K, i.e., at temperatures much lower than the other ones (95—108 K). The value of the relaxation times at 77 K was about 270 days. Because at low pressures the observed kinetics is exponential, it was possible to determine such

a long relaxation time from the measurement carried out only for 18 days. The initial value of the free-electron concentration was $n_0 = 9.7 \times 10^{12}$ cm^{-3}. After 18 days n reached the value 1.7×10^{13} cm^{-3}, while its equilibrium value, measured without application of pressure, was $n = 1.2 \times 10^{14}$ cm^{-3}. All the experimental points from Fig. 3 very well lie on the straight line for over 5 orders of magnitude, which gives evidence that τ is thermally activated with the activation energy well defined in the whole temperature range. As it has already been mentioned, at atmospheric pressure the observed kinetics is the emission of electrons from level B, which is degenerate with the conduction band. The result is that despite of its degeneration with the conduction band, the electron emission rate of level B is also thermally activated. Moreover, extremely long relaxation times τ, at low temperatures, mean on extremely small electron emission rate of level B—degenerate with the conduction-band continuum.

III. ANALYSIS OF THE EXPERIMENTAL RESULTS

The values of the relaxation time τ, where

$$\frac{1}{\tau} = -\lim_{n \to n_\infty} \frac{d}{dt} \ln | n(t) - n_\infty | ,$$

give information about the electron capture and emission processes controlled by level B. Relations between the values of the relaxation time τ and the electron capture cross section σ (or the emission rate α), are given below [see the formulas (A9) and (A3) in Appendix A]:

$$\sigma = \left[\tau \langle v \rangle (N_{CA} + N_{CB}) \times \frac{2n_\infty + N_a - N_d + N_{CX}}{2n_\infty + N_a - N_d + N_{CA}} \right]^{-1} , \quad (1)$$

$$\alpha = \sigma \langle v \rangle N_{CB} , \quad (2)$$

where σ is the total electron capture cross section of level B, including two possible channels of capture: direct transition (conduction band$\rightarrow$level B) and indirect transition via level A (conduction band$\rightarrow$level $A \rightarrow$level B). α is the total electron emission rate of level B, including two possible channels described above. $\langle v \rangle = (3kT/m^*)^{1/2}$ denotes the mean thermal velocity of free electrons, where m^* is the pressure- and temperature-dependent effective mass (calculations based on Refs. 5—7). n_∞ is the equilibrium value, pressure and temperature dependent, of the free-electron concentration. N_d and N_a are the concentrations of additional, always ionized donors and acceptors. $N_d - N_a$, as well as the X defect concentration N_x, is directly obtained from experiment. Also,

$$N_{CA} = \frac{1}{g_A} N_C \exp \frac{\epsilon_A}{kT} ,$$

$$N_{CB} = \frac{1}{g_B} N_C \exp \frac{\epsilon_B}{kT} ,$$

where

$$N_C = 2 \left[\frac{2\pi kTm^*}{\hbar^2} \right]^{3/2}$$

denotes the conduction-band density of states, and

$$N_{CX} = N_{CA} N_{CB} (N_{CA} + N_{CB})^{-1} .$$

ϵ_A, ϵ_B, g_A, and g_B denote the energies and the degeneration factors of levels A and B, respectively.

Following the paper of Kończykowski *et al.*[1] it was understood that $\epsilon_A = 85$ meV $- 10.5 \times 10^{-2}$ meV/MPa $\times p$, $\epsilon_B = 140$ meV $- 20 \times 10^{-2}$ meV/MPa $\times p$, and $g_A = g_B = 2$. ϵ_B was determined within the temperature range 116—148 K and the temperature dependence of ϵ_B appeared to be negligible. ϵ_A was determined only at 77 K but the value of ϵ_A plays a much less important role in Eq. (1) than ϵ_B does. Therefore, it is possible to assume that ϵ_A is also temperature independent. Kończykowski and co-workers[1-3] calculated the values of ϵ_A and ϵ_B, adopting statistics which did not take into consideration the vibronic states, and they assumed that $g_A = g_B = 2$. Hence ϵ_A and ϵ_B were estimated with certain errors (see Appendix

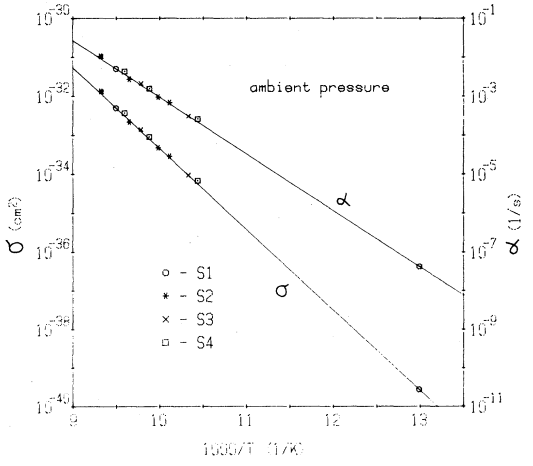

FIG. 4. Capture cross section σ and the emission rate α vs inverse temperature, recalculated from the values of τ presented in Fig. 3. The solid lines are the results of the fitting.

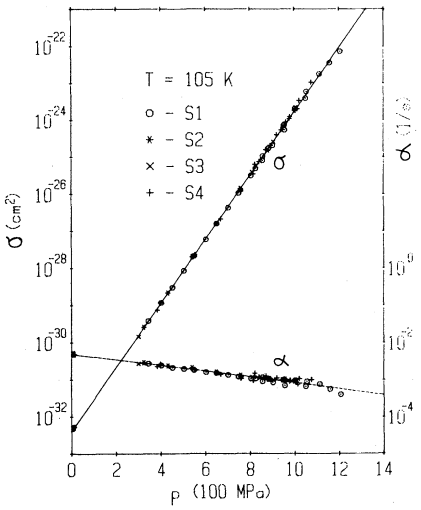

FIG. 5. Capture cross section σ and the emission rate α vs pressure, recalculated from the values of τ presented in Fig. 2. The solid lines are fitted.

B). However, consequent application of the same statistics as used by Kończykowski *et al.*, together with their values of ϵ_A and ϵ_B, did not lead to any errors in the determination of σ and α parameters.

Equations (1) and (2) enabled us to calculate σ and α from the experimental values of τ. Figure 4 presents $\log_{10}\sigma$ and $\log_{10}\alpha$ versus inverse temperature, recalculated from the values of τ presented in Fig. 3. All the points lie on straight lines. It means that σ as well as α are thermally activated with certain activation energies E_σ and E_α, given by the slopes of the lines. Figure 5 shows the pressure dependences of $\log_{10}\sigma$ and $\log_{10}\alpha$ recalculated from the values of τ shown in Fig. 2. The values of σ and α are the same for all the samples, despite differences in the values of τ seen in Fig. 2. It means that σ and α are characteristic for defect-center and host material and their values do not depend on the defect concentration N_x and sample compensation. The linear dependences of $\log^{10}\sigma$ and $\log_{10}\alpha$ upon pressure, presented in Fig. 5, mean that the activation energies E_σ and E_α are linear functions of pressure. The values of σ, calculated from Eq. (1), can be well described by the following expression:

$$\sigma=\sigma_\infty \exp\left[\frac{-E_\sigma(p=0)-(\partial E_\sigma/\partial p)p}{kT}\right], \tag{3}$$

where $\sigma_\infty=3\times10^{-13}$ cm^2, $E_\sigma(p=1)=413$ meV, and $\partial E_\sigma/\partial p=-18\times10^{-2}$ meV/MPa.

The values of $\partial E_\sigma/\partial p$ and $E_\sigma(p=0)$ are given by the slopes of the lines presenting $\log_{10}\sigma$ versus pressure (Fig. 5) and $\log_{10}\sigma$ versus inverse temperature (Fig. 4), respectively. It is worth pointing out that Eq. (1) permits two possible channels of capture: direct transition from the conduction band to level B and indirect transition via level A. Therefore, σ is a sum of two components (see Appendix A). From the other point of view, as it follows from the experiment, this sum is an exponential function given by Eq. (3). It means that only one of the two theoretically possible capture channels is active. We suppose that this is the indirect one, although the obtained results are insufficient to judge this problem. Solid lines in Fig. 4 and Fig. 5 were calculated from Eq. (3)—$\sigma(p,T)$ as well as Eqs. (2) and (3)—$\alpha(p,T)$ with the values of σ_∞, $E_\sigma(p=0)$, and $\partial E_\sigma/\partial p$ given above. In order to calculate $\alpha(p,T)$, instead of Eqs. (3) and (2) one can use the formula which is analogous to Eq. (3):

$$\alpha=\alpha_\infty \exp\left[\frac{-E_\alpha(p=0)-(\partial E_\alpha/\partial p)p}{kT}\right], \tag{4}$$

where $\alpha_\infty=3.5\times10^{11}$ s^{-1}, $E_\alpha(p=0)=289$ meV, and $\partial E_\alpha/\partial p=1.6\times10^{-2}$ meV/MPa.

By means of Eq. (3) and Eq. (1) it is possible to calculate the relaxation time τ for every sample and any pressure and temperature conditions. Solid lines in Figs. 2, 3, 6, and 7 were calculated in the above-mentioned manner. Figure 6 depicts experimental and theoretical pressure dependences of the relaxation time τ for sample $S4$ at temperatures $T=98.3$ K and $T=105$ K. Figure 7 shows experimental and theoretical temperature dependences of the relaxation time τ for sample $S2$ at some values of pressure. As it is obvious from

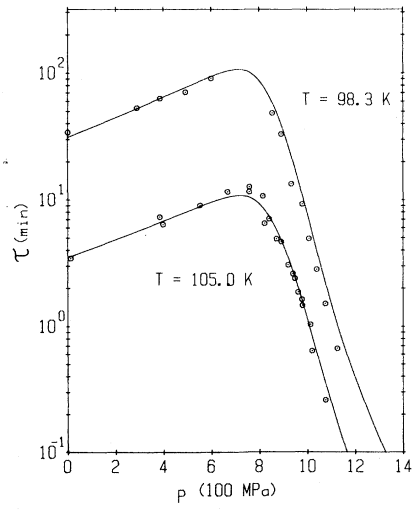

FIG. 6. Pressure dependences of the relaxation time τ measured for sample $S4$ at temperatures $T=105$ K and $T=98.3$ K. The solid lines are calculated.

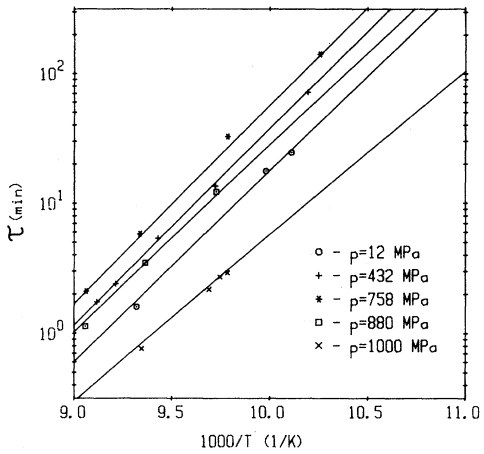

FIG. 7. Relaxation time vs inverse temperature measured for sample $S2$ at various values of pressure. The solid lines are calculated.

Figs. 2, 3, 6, and 7, in the whole temperature and pressure ranges, Eqs. (1)–(4) well describe the observed kinetics. The results obtained within the frame of the reported work show that in the whole range of applied pressures, the capture cross section σ and the emission rate α are thermally activated with large activation energies. Particularly interesting is that the electron emission rate is thermally activated even for level B being resonant ($p<700$ MPa) and the capture cross section is thermally activated even when level B lies below the bottom of the conduction band ($p>700$ MPa). Because σ and α are thermally activated, they reach extremely small values at low temperatures, e.g., at atmospheric pressure level B lies 140 meV above the bottom of the conduction band but at $T=77$ K the emission rate of this level is about 4.2×10^{-8} s^{-1}. Unusually small values of σ and α at low temperatures as well as their smooth pressure dependences (without any deflection at pressure at which level B enters the energy gap—see Fig. 5) prove that the interaction between level B and the conduction band is negligible. Thermal activation of σ and α and very effective quenching of the interaction between level B and conduction states are the results of strong coupling between level B and the crystal lattice.

IV. CONCLUSIONS

The following results obtained in the present work for n-InSb confirm strong coupling between the local level, level B, and the crystal lattice:

(1) The electron capture cross section σ and the electron emission rate α are thermally activated with large activation energies both at low pressures, at which level B is degenerate with the conduction band, and at high pressures, at which level B lies in the gap.

(2) At low temperatures σ and α reach extremely small values, inexplicable within any purely electronic model[8–10] (e.g., at $T=77$ K and $p=700$ MPa, at which level B lies at the bottom of the conduction band, $\alpha=6\times10^{-9}$ s^{-1} and $\sigma=4\times10^{-32}$ cm^2).

(3) Pressure dependences of σ and α are smooth and do not exhibit any deflection or other distinctive feature at the pressure at which level B enters the energy gap.

The last two facts mean that there is practically no interaction between level B and the band-states continuum (the interaction is markedly quenched by the strong coupling between level B and the crystal lattice).

In the case of n-InSb the coupling between X-defect and lattice vibrations can be qualitatively described by the configuration coordinate diagram shown in Fig. 8. This diagram is drawn for the case of level B lying below the bottom of the conduction band, i.e., for pressures $p>700$ MPa. The picture presents the adiabatic potential curves of the defect center in E-Q coordinates, where E is the total energy of the system (electronic plus elastic energy) and Q is the configuration coordinate. The curve $U_{c.b.}$ corresponds to the ionized defect, with the electron at the bottom of the conduction band, while the curves U_A and U_B correspond to the neutral defect with the electron localized on level A or B, respectively. Quantization of the sys-

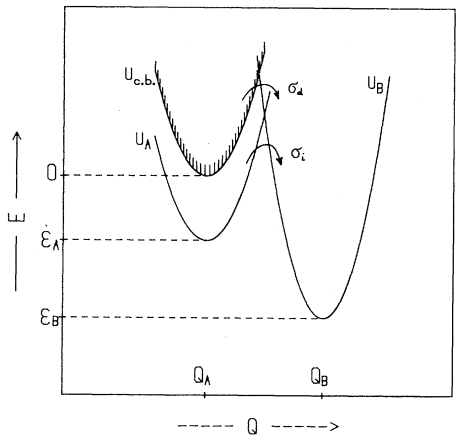

FIG. 8. Configuration coordinate diagram of the X defect in n-InSb drawn for the case of $p>700$ MPa.

tem movement in Q space causes the stationary states to be vibronic states of the potentials $U_{c.b}$, U_A, and U_B. The electron transitions between the conduction band and level B or between level A and level B are associated with the change of the system configuration $Q_A \rightleftarrows Q_B$. There are two theoretically possible channels of the capture of free electrons by level B—direct transition from the conduction band to level B (σ_d) and indirect transition via level A (σ_i). In both transitions there are adiabatic potential barriers to overcome. These barriers are responsible for very strong temperature dependences of electron capture cross section and electron emission rate of level B—irrespective of the energy position of level B. At sufficiently high temperatures or in the case of a wide barrier which is difficult to tunnel, the transitions take place practically above the top of the barrier, the so-called Mott limit. If so, the capture cross section σ is thermally activated and can be described by the following expression:

$$\sigma=\sigma_\infty \exp\left[-\frac{E_\sigma}{kT}\right], \tag{5}$$

where E_σ is the geometrical height of the barrier overcome in the capture process. Similar expression can be written for the emission rate α. In the case of the simple model with one-dimensional configuration coordinate Q and harmonic adiabatic potentials — (see Fig. 8) the barrier is relatively narrow and tunneling is an ordinary transition process—the Mott limit is not reached.[11–14] The exponential tails of vibronic wave functions, corresponding to the configurations Q_A and Q_B, overlap inside the barrier, which controls the probability of the tunneling process. The higher the energy of the initial vibronic state the smaller is its population (Boltzman factor) but the larger is the overlap of the initial-and final-state wave functions (narrower and lower barrier). Hence for some energy, lower than the true geometrical barrier height, the tunneling transitions are most effective. Because of the temperature-dependent Boltzman factor, this energy decreases with decreasing temperature.[13,14] So, if tunnel transitions are effective, then Eq. (5) is, in principle, not valid. This type of formula can be used only locally, within small temperature ranges.

However, in this case, (1) the activation energy E_{act} must be lower than the barrier geometrical height E_σ (or E_α) and it must depend on temperature, and (2) the preexponential factor must be much smaller than σ_∞ (or α_∞) because it is the product of σ_∞ (or α_∞) and the probability of the barrier tunneling at the energy equals E_{act}. The experimental results of the present work reveal none of the above-mentioned features characteristics for tunneling processes. In contrast, we conclude the following:

(1) The $\log\sigma$ $(1/T)$ and $\log\alpha$ $(1/T)$ dependences are linear in the whole range of applied temperatures (77 – 108 K) in which σ and α change 8 and 6 orders of magnitude, respectively. It means that activation energies of the capture cross section E_σ and of the emission rate E_α are constant in the whole temperature range (in CdF_2:In, because of tunneling, the activation energy changes by a factor of 1.7 in the similar temperature range).[12] Moreover, it is worth pointing out that activation energies E_σ and E_α are very large even at low temperatures at which σ and α are extremely small — which is unexpected in the case of effective tunneling transitions.[13]

(2) The experimental value of the preexponential factor in the $\sigma(T)$ dependence, obtained in this work, is very large ($\sigma_\infty = 3\times 10^{-13}$ cm^2). It is over an order of magnitude larger than the values of σ_∞ typical for defects which are strongly coupled to the lattice vibrations and which capture electrons in a nonradiative process of multiphonon emission in GaAs and GaP.[13,15]

All the above means that the adiabatic potential barrier must be very extensive, so that even at the lowest temperatures it is overcome above its geometrical height. The conclusion is that the capture or the emission of electron by level B leads to drastic local rearrangement of the crystal lattice (e.g., creation or annihilation of a defect complex or large defect motion in the crystal lattice). Moreover, harmonic approximation of adiabatic potentials may be used only in the neighborhood of the potential extrema and its extrapolation till the barrier area is unreasonable. Information about the barrier height and its pressure coefficient, obtained in this work, concern this area of the adiabatic potentials which is far from their extrema and is accessible only through kinetics study. These data can be of crucial importance for verification of the detailed X-defect model. However, the complete identification and the symmetry of this defect center is still unknown. Hence, it is not possible to present any reliable microscopic model of this center. On the other hand, Kończykowski *et al.*[1] considered level B in n-InSb to be "associated with the subsidiary X minimum of the conduction bands." Such identification was done because

the values of the pressure coefficients $\partial\epsilon_B/\partial p$ and $\partial\epsilon_{X\Gamma}/\partial p$ (where $\epsilon_{X\Gamma}=\epsilon_X-\epsilon_{\Gamma_6}$ is the energy separation between X and Γ_6 conduction-band minima) were similar. The same was the case with the local level of sulphur impurity, strongly coupled to the lattice vibrations in GaSb.[16,17] However, in the case of strong defect-lattice coupling, the thermal ionization energy cannot be purely electronic. Therefore, because the values of $\partial\epsilon_B/\partial p$ and $\partial\epsilon_X/\partial p$ are similar, two possible configurations of the defect center in n-InSb, as well as in GaSb:S, must correspond to almost the same crystal volume. In this case the contribution to $\partial\epsilon_B/\partial p$, originating from the crystal-volume changes, is small and the value of $\partial\epsilon_B/\partial p$ is almost entirely determined by a purely electronic component. This is quite different than for CdF_2:In, where the changes of the defect configuration mean the isotropic lattice distortion around the impurity atom and lead to large (about 25%) changes of the elementary cell volume.[12] CdF_2:In is, however, an ionic crystal and the interaction between the impurity and the crystal lattice should be quite different than in such crystals as InSb or GaSb.

APPENDIX A

If in the n-type semiconductor there is the metastable localized electron state, it is possible to observe the process in which free-electron concentration tends slowly to its equilibrium value. In order to find the relation between the relaxation time of the free-electron concentration τ and the electron capture cross section σ or the electron emission rate α, let us consider the system presented in Fig. 9. The characteristic features of the system are as follows:

(1) Both level A and B originate from an X-defect center, where the concentration is N_x.

(2) Level A is always in equilibrium with the conduction band, while level B is responsible for the observed slow kinetics.

(3) The kinetic equation considers level-A $\rightleftarrows$ level-B transitions and conduction-band $\rightleftarrows$ level-B transitions (both marked in Fig. 9 with arrows).

(4) Beside levels A and B there are additional following local electron levels being always in equilibrium with the conduction band: (a) donor level D of N_D concentration where the occupation by electrons changes during the relaxation process, and (b) always ionized donor and acceptor levels of N_d and N_a concentrations, respectively.

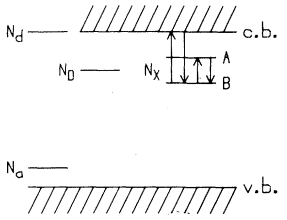

FIG. 9. Electronic levels considered in the analysis of the kinetics.

(5) Electron population in the conduction band can be described with Boltzman statistics (the Fermi level lies always sufficiently low).

Basic equations are the charge balance equation

$$n+n_A+n_B+n_D=N_x+N_D+N_d-N_a \ , \tag{A1}$$

and the kinetic equation

$$\frac{dn_B}{dt}=nN_x^+\sigma_B\langle v\rangle-n_B\alpha_B+n_A\varphi_A-n_B\varphi_B \ , \tag{A2}$$

where n is the free-electron concentration, n_A is the electron population of level A, n_B is the electron population of level B, n_D is the electron population of level D, $N_x^+=N_x-n_A-n_B$ denotes the concentration of nonoccupied X defect centers, σ_B is the electron capture cross section of level B, α_B is the electron emission rate of level B, φ_A is the probability of the electron transition from level A to level B, related to the unit of time, φ_B is the probability of the electron transition from level B to level A, related to the unit of time, and $\langle v\rangle$ is the mean thermal velocity of free electrons.

Let us leave the free-electron concentration n as the only time-dependent variable in Eq. (A2): (1) n_B must be ruled out by means of the charge-balance equation (A1) because level B is not always in equilibrium with the conduction band, and (2) n_A and n_D may be expressed directly by n from the general formula valid in the case when a defect center can have more than one electron levels[18]:

$$n_j=\frac{nN^+}{(1/g_j)N_C\exp(\epsilon_j/kT)} \ ,$$

where index j numbers the successive levels of the defect center, g_j is the degeneration of the level with the energy ϵ_j and N_C is the conduction-band density of states.

Furthermore, α_B and φ_B are related by detailed balance to σ_B and φ_A, respectively:

$$\alpha_B = N_{CB}\langle v\rangle\sigma_B \ , \tag{A3}$$

$$\varphi_B = \frac{N_{CB}}{N_{CA}}\varphi_A \ , \tag{A4}$$

where

$$N_{CA} = \frac{1}{g_A}N_C\exp\left[\frac{\epsilon_A}{kT}\right] ,$$

$$N_{CB} = \frac{1}{g_B}N_C\exp\left[\frac{\epsilon_B}{kT}\right] .$$

Thus the equation for dn/dt is as follows:

$$\frac{dn}{dt} = -\left[\sigma_B + \frac{\varphi_A}{\langle v\rangle N_{CA}}\right]\langle v\rangle \times (N_{CA}+N_{CB})\frac{F(n)}{G(n)} \ , \tag{A5}$$

where

$$\frac{F(n)}{G(n)} = \frac{n^2+(N_a-N_d+N_{CX})n - N_D N_{CD}\dfrac{n+N_{CX}}{n+N_{CD}} - N_{CX}(N_X+N_d-N_a)}{2n+N_a-N_d+N_{CA}+\dfrac{N_D N_{CD}(N_{CA}-N_{CD})}{(n+N_{CD})^2}} ,$$

$$N_{CD} = \frac{1}{g_D}N_C\exp\left[\frac{\epsilon_D}{kT}\right] ,$$

and

$$N_{CX} = \frac{N_{CA}N_{CB}}{N_{CA}+N_{CB}} .$$

The expression $\sigma_B+\varphi_A/(\langle v\rangle N_{CA})$ has a meaning of the total capture cross section of level B, σ, including two possible capture channels—direct and indirect via level A—σ_B and $\varphi_A/(\langle v\rangle N_{CA})$, respectively. The total capture cross section σ is related to the total emission rate α by the formula

$$\alpha = N_{CB}\langle v\rangle\sigma \ , \tag{A6}$$

which is similar to Eq. (A3). At thermal equilibrium, i.e., for $n=n_\infty$ where $n_\infty=\lim_{t\to\infty}n(t)$ there is $(dn)/(dt)\,|_{n=n_\infty}=0$ and function $F(n)$ from Eq. (A5) is equal to zero $[F(n_\infty)=0]$. If $F(n_\infty)$ is subtracted from $F(n)$, the factor $(n-n_\infty)$ can be easily excluded and Eq. (A5) takes the following form:

$$\frac{d}{dt}\ln|n-n_\infty| = -\sigma\langle v\rangle(N_{CA}+N_{CB})\left[\frac{n+n_\infty+N_a-N_d+N_{CX}+\dfrac{N_D N_{CD}(N_{CX}-N_{CD})}{(n+N_{CD})(n_\infty+N_{CD})}}{2n+N_a-N_d+N_{CA}+\dfrac{N_D N_{CD}(N_{CA}-N_{CD})}{(n+N_{CD})^2}}\right] . \tag{A7}$$

Because the right-hand side of Eq. (A7) depends on the free-electron concentration n, the time dependence of n is not, generally speaking, an exponential function. However, if there are no D donors ($N_D=0$), then for compensated samples (large $|N_a-N_d|$) $n(t)$ can be practically exponential. D donors cause, the kinetics to be nonexponential even for large $|N_a-N_d|$.

Let us consider two following simplified forms of Eq. (A7):

(1) The X defect center gives only one electron level—level B. Such a situation is equivalent to the limit $N_{CA}\to\infty$. Then Eq. (A7) has the following form:

$$\frac{d}{dt}\ln|n-n_\infty| = -\sigma_B\langle v\rangle\frac{n+n_\infty+N_a-N_d+N_{CB}+\dfrac{N_D N_{CD}(N_{CB}-N_{CD})}{(n+N_{CD})(n_\infty+N_{CD})}}{1+N_D N_{CD}/(n+N_{CD})^2} . \tag{A8}$$

Equation (A8) is equivalent to the formula used for GaSb:S by Dmowski *et al.*[19] The samples used by the authors were compensated and the nonexponential character of the observed kinetics was attributed to additional D donors.

(2) The X defect center possesses two electron levels—A and B, but there are no D donors ($N_D=0$). Then Eq. (A7) has the following form:

$$\frac{d}{dt}\ln|n-n_\infty| = -\sigma\langle v\rangle(N_{CA}+N_{CB})\frac{n+n_\infty+N_a-N_d+N_{CX}}{2n+N_a-N_d+N_{CA}} . \tag{A9}$$

Equation (A9) is useful for the case of n-InSb, which the present work refers to. For weakly compensated samples $|N_a-N_d| \ll n$ one can expect the nonexponential kinetics—if only N_{CA} is small. On the other hand, small N_{CA} means that level A lies deeply in the gap, which takes place at pressures $p \gg 700$ MPa.

Equations (A7)–(A9) allow us to obtain the values of the capture cross section σ or of the emission rate α from the experimental values of the relaxation time τ

$$\frac{1}{\tau} = -\lim_{n\to n_\infty}\frac{d}{dt}\ln|n-n_\infty| .$$

In this case it is necessary to have information about the energies and concentrations of the appropriate defect levels.

APPENDIX B

Statistics which take into account the vibronic states of X defect centers in n-InSb can be obtained on the basis of the canonical Gibbs distribution for the system with a variable number of particles. The probability of the occupation of a defect center by j electrons is equal[18,20]:

$$f_j = \frac{\gamma_j \exp\left[\dfrac{j\epsilon_F-\epsilon_j}{kT}\right]}{\displaystyle\sum_{n=0}^{N}\gamma_n\exp\left[\frac{n\epsilon_F-\epsilon_n}{kT}\right]} , \qquad \gamma_j = \sum_{m=0}^{r_j}\beta_{jm}\exp\left[-\frac{\epsilon_{jm}}{kT}\right] \tag{B1}$$

where j numbers the possible charge states of the defect center, f_j is the probability of finding the defect center with j electrons captured, ϵ_j is the ground-state energy of the defect center with j electrons, m numbers the possible excited states, ϵ_{jm} are the energies of the excited states with j electrons, related to the appropriate ground-state energy, and β_{jm} are the degeneration factors of the excited states with j electrons.

Figure 10 presents the situation characteristic for the X center in n-InSb:

(1) There are two charge states with $j=0$ and $j=1$.

(2) For $j=0$ there is an infinite ladder of vibronic excited states with energies $\epsilon_{0m}=m\hbar\omega_A$.

(3) For $j=1$ there are two infinite ladders of vibronic excited states with energies

$$\epsilon^B_{1m}=m\hbar\omega_B$$

and

$$\epsilon^A_{1m}=m\hbar\omega_A+(\epsilon_A-\epsilon_B) .$$

ϵ_B is the energy of the ground state of the defect with one electron ($j=1$).

(4) Degeneration factors β_{jm} are $\beta_{0m}=g^A_0$, $\beta^A_{1m}=g^A_1$, and $\beta^B_{1m}=g^B_1$.

Hence,

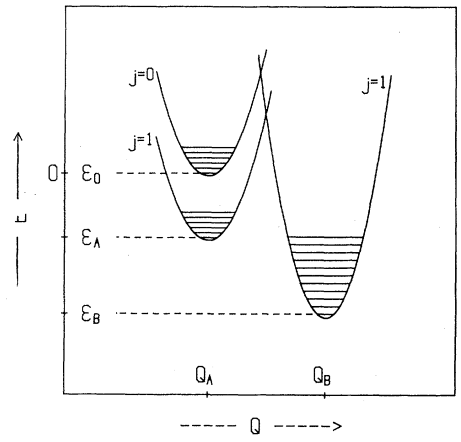

FIG. 10. Configuration coordinate diagram of the X defect in n-InSb illustrating the vibronic states taken into account in the statistics.

$$\gamma_0=\sum_{m=0}^{\infty} g_0^A \exp\left[\frac{m\hbar\omega_A}{kT}\right]$$
$$=\frac{g_0^A}{1-\exp\left[-\frac{\hbar\omega_A}{kT}\right]},$$
$$\gamma_1=\gamma_1^A=\gamma_1^B,$$
$$\gamma_1^A=\sum_{m=0}^{\infty} g_1^A \exp\left[-\frac{m\hbar\omega_A+\epsilon_A-\epsilon_B}{kT}\right]$$
$$=\frac{g_1^A \exp\left[\frac{\epsilon_B-\epsilon_A}{kT}\right]}{1-\exp(-\hbar\omega_A/kT)},$$
$$\gamma_1^B=\sum_{m=0}^{\infty} g_1^B \exp\left[-\frac{m\hbar\omega_B}{kT}\right]$$
$$=\frac{g_1^B}{1-\exp(-\hbar\omega_B/kT)}.$$

For the state with one electron ($j=1$), the probabilities of the ladder A and ladder B occupations are, respectively,

$$f_1^A=f_1\frac{\gamma_1^A}{\gamma_1},\quad f_1^B=f_1\frac{\gamma_1^B}{\gamma_1}.$$

Hence, the final formulas are

$$f_1^A=\frac{1}{\frac{g_0^A}{g_1^A}\exp\left[\frac{\epsilon_A-\epsilon_F}{kT}\right]+\frac{g_1^B}{g_1^A}\exp\left[\frac{\epsilon_A-\epsilon_B'}{kT}\right]+1},$$
$$f_1^B=\frac{1}{\frac{g_0^A}{g_1^B}\exp\left[\frac{\epsilon_B'-\epsilon_F}{kT}\right]+\frac{g_1^A}{g_1^B}\exp\left[\frac{\epsilon_B'-\epsilon_A}{kT}\right]+1}, \quad \text{(B2)}$$

where

$$\epsilon_B'=\epsilon_B+\Delta\epsilon,$$
$$\Delta\epsilon=kT\ln\frac{1-\exp\left[-\frac{\hbar\omega_B}{kT}\right]}{1-\exp\left[-\frac{\hbar\omega_A}{kT}\right]}.$$

The expressions (B2) have identical form as simple formulas, which do not take into account the vibronic states $\hbar\omega_A$ and $\hbar\omega_B$, with the only difference being that here, instead of ϵ_B we have ϵ_B'. Therefore, the use of the simple statistics, instead of the one given by Eq. (B2), is equivalent to the identification of the level-B thermal ionization energy with ϵ_B', instead of its real value ϵ_B. However, it does not lead to any formal inconsistency but only modifies the sense of the level-B energy. If $\omega_A=\omega_B$, then $\Delta\epsilon=0$ and vibronic states have no influence on the statistics form. For $0.3 \leq \omega_A/\omega_B \leq 3$ the magnitude of $\Delta\epsilon$ does not exceed $\pm kT$.

*On leave from Physics Laboratory I, University of Patras, Patras, Greece.

[1]M. Kończykowski, S. Porowski, and J. Chroboczek, *Proceedings of the Eleventh International Conference on the Physics of Semiconductors,* edited by M. Miasek (PWN—Polish Scientific, Warsaw, 1972), Vol. 2, p. 1050.

[2]S. Porowski, M. Kończykowski, and J. Chroboczek, Phys. Lett. 48A, 189 (1974).

[3]S. Porowski, M. Kończykowski, and J. Chroboczek, Phys. Status Solidi B 63, 291 (1974).

[4]L. Dmowski, M. Kończykowski, R. Piotrzkowski, and S. Porowski, Phys. Status Solidi B 73, K131 (1976).

[5]C. R. Pidgeon and R. N. Brown, Phys. Rev. 146, 575 (1966).

[6]H. M. Abduvahidov, A. S. Volkov, and V. V. Galavanov, Fiz. Tverd. Tela (Leningrad) 4, 1409 (1970).

[7]H. Ehrenreich, J. Phys. Chem. Solids 2, 131 (1957).

[8]A. Sklensky and R. H. Bube, Phys. Rev. B 6, 1328 (1972).

[9]R. J. Keyes, J. Appl. Phys. 38, 2619 (1967).

[10]D. L. Losee, R. P. Khosla, D. K. Ranadive, and F. T. J. Smith, Solid State Commun. 13, 819 (1973).

[11]R. Pässler, Phys. Status Solidi B 85, 203 (1978).

[12]J. M. Langer, U. Ogonowska, and A. Iller, in *Proceedings of the Fourteenth International Conference on the Physics Semiconductors, Edinburgh, 1978,* edited by B. L. H. Wilson (Institute of Physics, Bristol, 1978).

[13]C. H. Henry and D. V. Lang, Phys. Rev. B 15, 989 (1977).

[14]J. M. Langer, in Proceedings of the Fifteenth International Conference on the Physics of Semiconductors Kyoto, 1980 [J. Phys. Soc. Jpn. 49, Suppl. A (1980)].

[15]There are two probable reasons for the extremely large value of σ_∞: The defect potential is attractive, and the change of the defect charge state is accompanied by the reorganization of the defect structure which is much larger than the one described by C. H. Henry and D. V. Lang.

[16]B. B. Kosicki, Harvard University Technical Report

No. HP-19, 1967 (unpublished).
[17]L. Dmowski, M. Baj, and S. Porowski, in *Proceedings of the High-Pressure and Low-Temperature Physics International Conference, Cleveland, Ohio, 1977* (Plenum, New York, 1978).
[18]J. S. Blakemore, *Semiconductor Statistics* (Pergamon, New York, 1972).
[19]L. Dmowski, M. Baj, M. Kubalski, R. Piotrzkowski, and S. Porowski, in *Proceedings of the Fourteenth International Conference on the Physics of Semiconductors, Edinburgh, 1978* (Institute of Physics, Bristol, 1979).
[20]V. L. Bonch-Bruyevich and S. G. Kalashnikov, *Fizika Poluprovodnikov* (Nauka, Moskva, 1977).